JOURNAL OF COLLOID AND INTERFACE SCIENCE **188,** 313–324 (1997)
ARTICLE NO. CS974719

Hydrodynamic Theory for Spontaneously Growing Dimple in Emulsion Films with Surfactant Mass Transfer

KRASSIMIR D. DANOV,* THEODOR D. GURKOV,*,[1] TATYANA DIMITROVA,* IVAN B. IVANOV,* AND DANIEL SMITH†

**Laboratory of Thermodynamics and Physico-Chemical Hydrodynamics, University of Sofia, Faculty of Chemistry, James Boucher Avenue 1, Sofia 1126, Bulgaria; and †DOW Deutschland, Inc., Industriestrasse 1, Postfach 20, D-77836 Rheinmuenster, Germany*

Received July 15, 1996; accepted December 2, 1996

In this paper we propose a theory for the recently discovered phenomenon of spontaneous cycling dimpling. The latter is responsible for the high stability of non-equilibrium aqueous emulsion films when surfactant is transferred across the interfaces toward the surrounding oil phases. Our treatment is based on the lubrication approximation for the thin film hydrodynamics, with account for the surfactant fluxes due to convection and diffusion. A fourth-order differential equation is derived for the time evolution of the surface shape. This equation is solved numerically, and the results are compared with experimental profiles (determined by means of interferometry). Very good agreement is observed. It is proved that the surface viscosity and the surface diffusion are insignificant for the dimple growth. Quite essential is the Marangoni effect: the exhaustion of surfactant from the region around the film center gives rise to gradients of the interfacial tension which set the interface into motion, and consequently, liquid is dragged into the film, feeding the dimple.

Key Words: **thin liquid films; mass transfer; surface flow; dimple growth; Marangoni effect.**

1. INTRODUCTION

The thin aqueous films between oil phases represent a convenient model system for investigations on the stability of oil-in-water dispersions. A film is formed when two emulsion droplets (of not very small size) approach toward each other. Until recently, relatively little effort has been spent to study the behavior of such films in non-equilibrium conditions, when surfactants or other solutes are being transferred from, to, or across the film. On the other hand, common non-ionic surfactants are often soluble both in water and in oil, and are initially put in one of the phases. Thus, immediately after formulation of the dispersion a process of surfactant redistribution starts. It can last for several hours, and even up to days, until the equilibrium is reached. This is a reason why the transient non-equilibrium phenomena can have important practical implications.

From a physical point of view, many different effects connected with the mass transfer may exist. Let us mention some of them briefly. The diffusion of acetic acid and acetone, directed from the surrounding oil phases toward the aqueous film, was studied experimentally in refs. (1, 2). Substantial destabilisation was observed, which could be a consequence of Marangoni–Gibbs instabilities. The latter manifest themselves in a growth of capillary waves at the interfaces, eventually causing film rupture. Such instabilities can appear on a single liquid surface as well, giving rise to spontaneous emulsification (3, 4).

In contrast to refs. (1, 2), very stable and thick films have been recently reported (5), in the case when *surfactant* is transferred from the oil to the film. The effect was attributed to osmotic swelling, due to the higher concentration of surfactant micelles in the film interior, compared to that in the aqueous meniscus. As the diffusion of the big micellar aggregates is slow, and the film diameter is much larger than its thickness, the osmotic pressure gradients force the liquid to rush from the Plateau border into the film (5). As a consequence, intensive circulation and exchange of mass with the meniscus take place and can be directly observed (5).

Diffusion of *solvent* (water) across lipid bilayers was found to be important for the stability of two apposed biomembranes against fusion (6). If the osmotic differences are such as to remove water from between the bilayers (more concentrated NaCl solution in the aqueous drops), then fusion occurs. In the opposite case, if there is an osmotic flow of water into the space between the membranes (the film), fusion never happens (6).

In general, the behavior of non-equilibrium films with mass transfer is quite complicated, and to a large extent specific, depending on what kind of substance is transferred, and to which direction. Each particular case is to be analyzed with care, since different physical effects may superimpose. Let us now concentrate on the situation when a surface active solute diffuses from the continuous phase (film) to the dispersed phase (oil), across the interfaces. As pointed out by Hartland (7), this should lead to stabilization. Because the volume of the film is small, the solute concentration there falls more rapidly than in the bulk of the continuous phase,

[1] To whom correspondence should be addressed. E-mail: theodor.gurkov@ltph.cit.bg.

0021-9797/97 $25.00

and hence, the interfacial tension is greater around the film center and smaller at the periphery and in the meniscus. A tensile restoring force emerges, which is directed opposite to the surfactant density gradient (8) (i.e., from higher to lower surface pressure). It sets the fluid interface into motion, and liquid is dragged toward the film center. This is a manifestation of the well-known Marangoni effect (7, 8) and is expected to provide high stability. Such a qualitative picture has been confirmed by recent experiments (9), and moreover, it turns out that the real processes are far more complex.

In the paper of Velev *et al.* (9) a fascinating cyclic phenomenon was encountered during observations of aqueous emulsion films between oil phases in the presence of nonionic surfactant (soluble both in water and in oil). When the surfactant is initially dissolved in the film phase and diffuses across the interfaces towards the oil, its transfer induces spontaneous growth of a lens-like thicker formation (dimple) around the film center. The thickness along the periphery remains more or less constant. Upon reaching a certain size, the dimple flows out into the meniscus, and a new one starts to form. The process is cyclic and usually goes on for many hours. Its driving force was proven to be the surfactant mass transfer (9). When the latter ceases, the film quickly thins down and eventually ruptures. In view of those findings, the phenomenon is likely to be responsible for the stability of emulsion systems with non-equilibrium distribution of surfactant. It should be noted that the films containing such dimples can be very thick, even in the presence of a large amount of added electrolyte (up to 300–400 nm with 0.1 *M* NaCl). No other sources of stabilization are operative in these conditions except purely hydrodynamic ones.

A clear distinction must be made between the cyclic dimpling reported in ref. (9) and the so-called hydrodynamic dimple (10, 11). The latter appears only when the film is thinning and is not connected in any respect with mass transfer through the phase boundaries. The film surfaces are curved under the action of the pressure gradients and the viscous friction. At a certain stage of thinning the hydrodynamic dimple irreversibly disappears and the film becomes plane-parallel. A comprehensive review of studies devoted to this phenomenon can be found in ref. (11). Recently Hartland *et al.* (12) have solved numerically the differential equation governing the shape as a function of time during the drainage of thin liquid films. In contrast to the hydrodynamic dimple, the cyclic dimple discovered in (9) has the following characteristic features: (i) it is driven entirely by the surfactant redistribution; (ii) the film region around the periphery does not thin at all; (iii) the processes go on in a cyclic manner for several hours, until the concentration reaches equilibrium.

The aim of this article is to develop a detailed theoretical description for the progressive growth of a cyclic dimple. We use the lubrication approximation for the thin film hydrodynamics and take into account the surfactant diffusion and fluxes. A differential equation for the time evolution of the interfacial shape is formulated and solved numerically. Comparison with experimentally determined profiles is carried out and very good agreement is observed. The analysis gives the possibility to figure out which physical properties of the system are relevant for the phenomenon.

2. MATHEMATICAL FORMULATION OF THE PROBLEM

Let S be the upper surface of a thin emulsion film with circular symmetry. It is defined by the following equation (see Fig. 1)

$$S: z = h(r, t), \qquad [1]$$

where t denotes time, and r and z are the radial and vertical coordinates in the cylindrical coordinate system $Or\varphi z$. R is the film radius; the thickness along the periphery is $h_0 = 2h$ $(r = R, t)$, and remains constant. We shall assume validity of the lubrication approximation, which states that $h(r, t) \ll R$. With the typical dimensions of the films this is always fulfilled (see below). In the lubrication theory the liquid flow is governed by the equations (see, e.g., ref. (13))

$$\frac{1}{r}\frac{\partial}{\partial r}(r\nu_r) + \frac{\partial \nu_z}{\partial z} = 0 \qquad [2]$$

$$\frac{\partial p}{\partial r} = \eta \frac{\partial^2 \nu_r}{\partial z^2}, \frac{\partial p}{\partial z} = 0 \qquad [3]$$

p is the pressure inside the film, η is the dynamic viscosity, and ν_r and ν_z are respectively the radial and vertical velocity components ($\nu_z \ll \nu_r$). We work at low Reynolds number, and in quasistatic approximation. The latter means that the derivatives $\partial/\partial t$ in the Navier–Stokes equations are neglected, and all physical quantities depend on time implicitly, through $h(r, t)$. Equations [2] and [3] can be integrated by using the kinematic boundary conditions on the surface S:

$$\nu_r = u, \nu_z = \frac{\partial h}{\partial t} + u\frac{\partial h}{\partial r} \quad \text{at } S \qquad [4]$$

where u is the radial component of the velocity at the surface. The solutions are symmetrical for positive and negative values of z, and in this case we can write the following conditions at the midplane of the film

$$\frac{\partial \nu_r}{\partial z} = 0, \nu_z = 0 \text{ at } z = 0. \qquad [5]$$

Ivanov and Dimitrov (11) have shown that the solution of the problem [2]–[5] is

$$p = q(r, t), \nu_r = \frac{1}{2\eta}\frac{\partial q}{\partial r}(z^2 - h^2) + u \qquad [6]$$

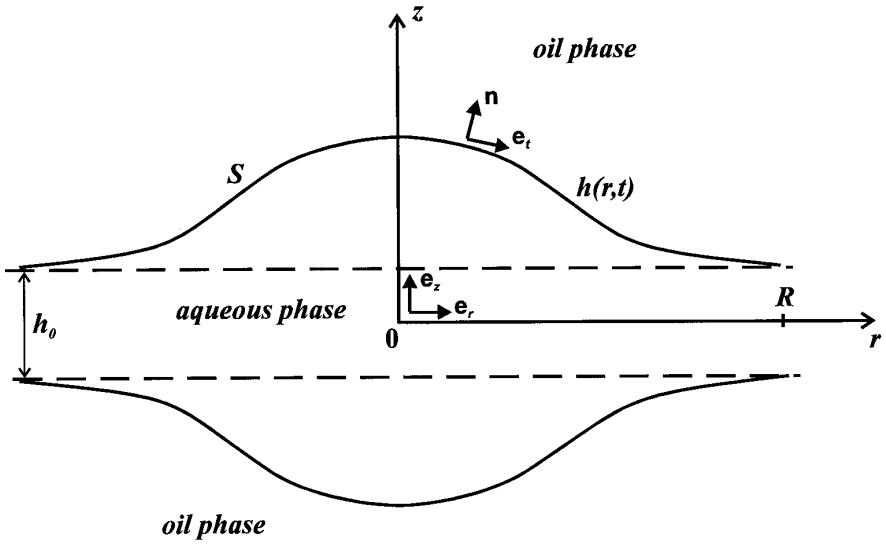

FIG. 1. Sketch of an emulsion film with dimple.

Here q is the pressure in the film (it does not depend on z). After integrating the continuity equation [2] from 0 to $h(r, t)$, using the conditions [4] and [5] for ν_z and inserting the general solution [6] for ν_r, we end up with the following equation for the shape of the interface S

$$\frac{\partial h}{\partial t} + \frac{1}{r}\frac{\partial}{\partial r}(rhu) = \frac{1}{3\eta r}\frac{\partial}{\partial r}\left(rh^3\frac{\partial q}{\partial r}\right) \qquad [7]$$

The unknown functions $u(r, t)$, $\partial q/\partial r$ in Eq. [7] have to be determined from the other boundary conditions at S.

The inertia terms have been discarded from the Navier–Stokes equations in the film, as the motion is slow. In the *oil* phase the balance between the viscous and the inertia terms leads to introducing a characteristic thickness of the layer within which the velocity changes significantly. As Stokes (14) and Lord Rayleigh (15) have shown (see also (13)), this thickness can be estimated as $\delta_\nu \approx \sqrt{\nu_0\tau}$, where ν_0 is the kinematic viscosity and τ is the time scale of the tangential motion. In our case τ coincides with the characteristic period of the oscillations. Hence, simple evaluation reveals that in the oil phase $\delta_\nu \approx 1$ cm $\gg h$, which means that the velocity gradients are negligible. Therefore, the viscous stresses from the side of the oil will not contribute to the balance of the surface stresses on S. On the other hand, Ivanov and Traykov (16) and Traykov and Ivanov (17) have observed a strong influence of the oil phase viscosity upon the process of thinning of an emulsion thin liquid film. However, in their case the characteristic time was much smaller than τ in the present problem, when oscillating dimple exists. In particular, $\delta_\nu \approx h$ for the systems studied in (16, 17).

In view of these considerations one can deduce that the balance of the tangential component of the stress tensor at the surface S acquires the following form (see the Appendix):

$$\eta\frac{\partial \nu_r}{\partial z} = \frac{\partial \sigma}{\partial r} + \eta_S\frac{\partial}{\partial r}\left[\frac{1}{r}\frac{\partial}{\partial r}(ru)\right] \text{ at } S. \qquad [8]$$

The balance of the normal component of the stress tensor on S yields

$$-\frac{\partial q}{\partial r} = \frac{\partial}{\partial r}\left[\frac{\sigma}{r}\frac{\partial}{\partial r}\left(r\frac{\partial h}{\partial r}\right) + \Pi(h)\right] \text{ at } S. \qquad [9]$$

In Eqs. [8] and [9], σ is the interfacial tension and η_S is a characteristic surface viscosity, which represents the sum of the dilatation and shear viscosities, $\eta_s = \eta_d + \eta_{sh}$ (cf. Appendix). $\Pi(h)$ is the disjoining pressure, whose origin is connected with different intermolecular interactions (electrostatic, van der Waals, etc.) leading to direct forces between the two film surfaces. Π is negligible for relatively thick films, say, for $h > \sim$100 nm. In the particular system analyzed in the next section of this paper $\Pi = 0$, but in principle there may exist thinner non-equilibrium films for which Π will be important.

We estimate the role of the surface viscosity taking the ratio of the respective terms in Eq. [8]:

$$\eta_S\frac{\partial}{\partial r}\left[\frac{1}{r}\frac{\partial}{\partial r}(ru)\right] \Big/ \left(\eta\frac{\partial \nu_r}{\partial z}\right) \approx \frac{\eta_S h_0}{\eta R^2}. \qquad [10]$$

Our parameters are $\eta_s \approx 10^{-3}$ surface poises (g/s), a value typical for low molecular weight surfactants (8), $\eta \approx 10^{-2}$ poises (water), $h_0 \approx 3.5 \times 10^{-5}$ cm, and $R \approx 3 \times 10^{-2}$ cm (see the next section). Then, the right-hand side of Eq. [10] gives 3.9×10^{-3}, which is much less than unity. One can draw the conclusion that the surface viscosity is insignificant. Then from Eqs. [6] and [8] we obtain a simpler boundary condition,

$$h\frac{\partial q}{\partial r} = \frac{\partial \sigma}{\partial r} \text{ at } S. \quad [11]$$

Equation [9] implies that $\partial p/\partial r$ was supposed to be zero in the oil phase, close to the interface (cf. Appendix, Eq. [A.6]). This is a reasonable assumption (11), since the motion in the oil is caused only by the moving surface which drags the adjacent liquid. Hence, the pressure gradients should be small.

Let us now consider the distribution of the surfactant concentration in the aqueous phase, $c(r, z, t)$. The diffusion equation in the volume of the film reads (11)

$$\frac{\partial c}{\partial t} + \nu_r\frac{\partial c}{\partial r} + \nu_z\frac{\partial c}{\partial z} = D\left[\frac{\partial^2 c}{\partial z^2} + \frac{1}{r}\frac{\partial}{\partial r}\left(r\frac{\partial c}{\partial r}\right)\right], \quad [12]$$

where D is the bulk diffusion coefficient. We introduce the following dimensionless variables:

$$\theta = \frac{t}{\tau},\ \rho = \frac{r}{R},\ \zeta = \frac{z}{h_0},\ U = \frac{\nu_r}{R/\tau},\ V = \frac{\nu_z}{h_0/\tau}. \quad [13]$$

Here τ denotes the time scale of dimple growth. According to Eq. [13], we can cast Eq. [12] into dimensionless form in terms of θ, ρ, ζ, U, and V:

$$\frac{\partial c}{\partial \theta} + U\frac{\partial c}{\partial \rho} + V\frac{\partial c}{\partial \zeta} = \frac{1}{Pe}\left[\frac{1}{\epsilon}\frac{\partial^2 c}{\partial \zeta^2} + \frac{1}{\rho}\frac{\partial}{\partial \rho}\left(\rho\frac{\partial c}{\partial \rho}\right)\right] \quad [14]$$

The small quantity ϵ is defined as $\epsilon = h_0^2/R^2$. The Peclet number is

$$\mathrm{Pe} = \frac{R^2}{D\tau} \quad [15]$$

For the characteristic parameters of the problem, $R \approx 3 \times 10^{-2}$ cm, $D \approx 5 \times 10^{-6}$ cm^2/s, and $\tau \approx 100$ s, one calculates Pe = 1.8, and therefore we have to consider the case when the Peclet number is not small. Bearing in mind that the film is being continuously fed with fresh liquid from the meniscus, it is natural to regard the solution of Eq. [14] as a slight perturbation to the concentration in the bulk aqueous phase, c_0. Further, it will be assumed that c_0 remains constant during the evolution of the dimple (see the discussion below). We seek a function $c(\rho, \zeta, \theta)$ in the form

$$c = c_0 + \epsilon c_1 + \epsilon^2 c_2 + \cdots \quad [16]$$

After substitution of Eq. [16] into Eq. [14], the terms which are of same order of magnitude with respect to ϵ can be equated. Thus, one obtains that c_1 depends only on ρ and θ, and

$$\frac{\partial^2 c_2}{\partial \zeta^2} = Pe\left(\frac{\partial c_1}{\partial \theta} + U\frac{\partial c_1}{\partial \rho}\right) - \frac{1}{\rho}\frac{\partial}{\partial \rho}\left(\rho\frac{\partial c_1}{\partial \rho}\right). \quad [17]$$

The condition for film symmetry leads to $\partial c/\partial \zeta = 0$ on the plane $\zeta = 0$.

We need Eq. [17] in order to determine the diffusion flux of surfactant, j_f, directed from the film toward the surface S. Up to linear order in $\partial h/\partial r$, j_f is given by

$$j_f = -D\mathbf{n}\cdot\nabla c|_{z=h} = -D\left(\frac{\partial c}{\partial z} - \frac{\partial h}{\partial r}\frac{\partial c}{\partial r}\right) \text{ at } S, \quad [18]$$

see Appendix, Eq. [A.2]. The two terms in the right-hand side of Eq. [18] are of comparable magnitude, because $\partial c/\partial r \gg \partial c/\partial z$ (cf. Eq. [16]), but $\partial h/\partial r$ is small. After integration of Eq. [17] from 0 to h/h_0 over ζ, using Eq. [6] to substitute for $U(\zeta)$, we return to the physical variables and find the value of the diffusion flux, j_f,

$$j_f = -h\frac{\partial c}{\partial t} - uh\frac{\partial c}{\partial r} + \frac{h^3}{3\eta}\frac{\partial q}{\partial r}\frac{\partial c}{\partial r} + \frac{D}{r}\frac{\partial}{\partial r}\left(rh\frac{\partial c}{\partial r}\right) \text{ at } S. \quad [19]$$

The characteristic distance of diffusion penetration in the oil phase is much greater than the film thickness. Hence, in zero approximation the diffusion flux into oil, j_0, does not depend on r and is of the order of the flux from the side of the film, j_f. Actually, the mass transfer between the phases will lead to a gradual change of both the bulk concentration, c_0, and the flux, j_0. This process can be analyzed by solving the diffusion problem in the system. In principle, there will be a slow change of all physical quantities related with c_0: the adsorption of surfactant, Γ_0, the interfacial elasticity, G_0, etc. However, it is experimentally established that this change goes on for many hours, i.e., it is very slow compared to the characteristic time of dimple growth, τ. We shall assume that during the evolution of a dimple, which takes times of the order of minutes, the parameters referring to c_0 (namely, j_0, Γ_0, and G_0) remain *constant.*

According to Eq. [16], the surfactant adsorption at the surface, Γ, can be expressed as an expansion:

$$\Gamma = \Gamma_0 + \left(\frac{\partial \Gamma}{\partial c}\right)_0 (c - c_0) \text{ at } S, \quad [20]$$

as far as we consider weak perturbations with respect to c_0. The adsorption is supposed to have reached its equilibrium value, Γ_0, for the corresponding c_0. Equation [20] is valid when local equilibrium is established at *any* moment of time between the adsorption layer and the subsurface where the concentration is c. Then Γ is an explicit function of c only. Such is the situation with diffusion controlled adsorption, which

is likely to be the case in our system, described in the next section, as we have non-ionic surfactant (no barrier for adsorption). The surfactant mass balance equation on S reads (11)

$$\frac{\partial \Gamma}{\partial t} + \nabla_{II}\cdot(\Gamma \mathbf{v}_S - D_S \nabla_{II}\Gamma) = j_f - j_0. \qquad [21]$$

Here D_S denotes the surface diffusivity; for the other symbols see the Appendix. When combined with Eqs. [7], [19], and [20], Eq. [21] yields

$$\frac{\partial}{\partial t}\left\{\left[\left(\frac{\partial \Gamma}{\partial c}\right)_0 + h\right](c - c_0)\right\} + \frac{1}{r}\frac{\partial}{\partial r} \times \left\{ru\left[\Gamma_0 + \left(\left(\frac{\partial \Gamma}{\partial c}\right)_0 + h\right)(c - c_0)\right]\right\} - \frac{1}{r}\frac{\partial}{\partial r}\left\{r\left[D_S\left(\frac{\partial \Gamma}{\partial c}\right)_0 + Dh\right]\frac{\partial (c - c_0)}{\partial r}\right\} - \frac{1}{r}\frac{\partial}{\partial r}\left[\frac{rh^3(c - c_0)}{3\eta}\frac{\partial q}{\partial r}\right] + j_0 = 0 \text{ at } S. \qquad [22]$$

The characteristic film thickness, $h_0 \approx 3.5 \times 10^{-5}$ cm, is much less than $(\partial\Gamma/\partial c)_0 \approx 1.3 \times 10^{-3}$ cm, the latter being estimated from the equilibrium interfacial tension isotherm of nonylphenol ethoxylate (with 40 ethylene oxide groups), close to CMC. In the quasistatic approximation, we neglect the time derivative (see above) and Eq. [22] acquires the form

$$\frac{1}{r}\frac{\partial}{\partial r}(ru\Gamma_0) - \frac{1}{r}\frac{\partial}{\partial r}\left\{r\left[D_S\left(\frac{\partial \Gamma}{\partial c}\right)_0 + Dh\right]\frac{\partial (c - c_0)}{\partial r}\right\} + j_0 = 0 \text{ at } S. \qquad [23]$$

It can be shown that the coefficient of surface diffusion, D_S, is greater than or of the same order as that in the bulk of the film, D (18). Hence, the term Dh in Eq. [23] may be discarded, and after integrating over r we obtain

$$u\Gamma_0 - D_S\left(\frac{\partial \Gamma}{\partial c}\right)_0 \frac{\partial (c - c_0)}{\partial r} + \frac{j_0 r}{2} = 0 \text{ at } S. \qquad [24]$$

In view of Eq. [16], at weak perturbations, one may represent the interfacial tension as

$$\sigma = \sigma_0 + \left(\frac{\partial \sigma}{\partial c}\right)_0 (c - c_0) \text{ at } S, \qquad [25]$$

where σ_0 is the value unperturbed by the dimple growth (i.e., at c_0). Inserting Eq. [25] into [11] and using Eq. [24] for the radial component of the velocity, u, we eliminate $(c - c_0)$ and arrive at the following relationship on the surface S

$$u = -\frac{D_S h}{G_0}\frac{\partial q}{\partial r} - \frac{j_0 r}{2\Gamma_0} \text{ at } S, \qquad [26]$$

where G_0 is the surface elasticity:

$$G_0 = -\left(\frac{\partial \sigma}{\partial \ln \Gamma}\right)_0. \qquad [27]$$

Now we substitute u in Eq. [7] with Eq. [26]. Comparing the terms which contain $\partial q/\partial r$, one encounters the dimensionless parameter

$$3\eta D_S/(G_0 h_0) = 9 \times 10^{-3} \ll 1,$$

with $G_0 = 10$ dyn/cm and $D_S = 10^{-4}$ cm^2/s. We conclude that the influence of the molecular surface diffusion is negligible. Hence, using Eq. [9] we derive the final form of the differential equation for the surface profile, $h(r, t)$,

$$\frac{\partial h}{\partial t} + \frac{1}{3\eta r}\frac{\partial}{\partial r}\left\{rh^3\frac{\partial}{\partial r}\left[\frac{\sigma_0}{r}\frac{\partial}{\partial r}\left(r\frac{\partial h}{\partial r}\right) + \Pi(h)\right]\right\} = \frac{j_0}{2\Gamma_0 r}\frac{\partial}{\partial r}(r^2 h). \qquad [28]$$

One can write the following boundary conditions for Eq. [28]:

$$\frac{\partial h}{\partial r}(r = 0, t) = 0 \text{ at } t \geqslant 0 \qquad [29]$$

$$h(r = R, t) = \frac{h_0}{2}, \frac{\partial h}{\partial r}(r = R, t) = 0 \text{ at } t \geqslant 0. \qquad [30]$$

The thickness of the film along the periphery, h_0, remains fixed. The fourth boundary condition can be found from the requirement that $\partial h/\partial t$ for $r = 0$ be finite at any moment of time. This gives

$$\frac{\partial^3 h}{\partial r^3}(r = 0, t) = 0 \text{ at } t \geqslant 0. \qquad [31]$$

It is possible to define the initial condition at $t = 0$ as a plane-parallel film of thickness h_0:

$$h(r, t = 0) = \frac{h_0}{2} \text{ at } 0 \leqslant r \leqslant R. \qquad [32]$$

In the general case only numerical solutions of the problem [28]–[32] can be obtained.

We would like to mention here that the formulated govern-

ing equations and the boundary conditions on the interface, S, are valid also in the meniscus region which is adjacent to the film (as long as the lubrication approximation retains its applicability). The experimental observations have revealed that the thickness at the film periphery remains constant during the evolution of a dimple. This gives us the opportunity to impose the boundary conditions, expressed by Eq. [30], along the rim. Thus, the hydrodynamic problem in the film is defined, and we avoid the necessity of considering explicitly the meniscus region.

3. NUMERICAL RESULTS AND COMPARISON WITH EXPERIMENT

We shall consider relatively thick films, $h_0 \approx 300$ nm and above, when the disjoining pressure, Π, can be disregarded. Equation [28] is cast into dimensionless form using Eq. [13].

$$\frac{\partial H}{\partial \theta} + \alpha \frac{1}{\rho}\frac{\partial}{\partial \rho}\left\{\rho H^3 \frac{\partial}{\partial \rho}\left[\frac{1}{\rho}\frac{\partial}{\partial \rho}\left(\rho \frac{\partial H}{\partial \rho}\right)\right]\right\} = \beta \frac{1}{\rho}\frac{\partial}{\partial \rho}(\rho^2 H), \quad [33]$$

where $H = h/h_0$, and the parameters α, β are defined as

$$\alpha = \frac{1}{3}\frac{\tau \sigma_0}{\eta}\frac{h_0^3}{R^4}, \beta = \frac{j_0 \tau}{2\Gamma_0}. \quad [34]$$

Equation [33] is a nonlinear partial differential equation of fourth order. The time and the radial coordinate are discretized with increments $\Delta\theta$, $\Delta\rho$, and a semi-implicit numerical scheme is employed (see, e.g., ref. (19)). The highest order derivatives are expressed at the time moment $(\theta + \Delta\theta)$, with central differences of accuracy $(\Delta\rho)^2$. The resulting linear set of equations is solved by Gauss–Jordan elimination with full pivoting. The point $\rho = 0$ needs special treatment. After expanding Eq. [33] in series at $\rho \to 0$, one finds

$$\frac{\partial H(0, \theta)}{\partial \theta} + \alpha \frac{8}{3}\left.\frac{\partial^4 H}{\partial \rho^4}\right|_{\rho=0} H^3(0, \theta) = \beta\left[2 H(0, \theta) + \left.\frac{\partial^2 H}{\partial \rho^2}\right|_{\rho=0}\right]. \quad [35]$$

It is evident that the solution ultimately depends on two parameters, α and β. In general, the profiles $H(\rho, \theta)$ exhibit a steady state after some characteristic time. Figure 2 illustrates this behavior. Computed shapes are plotted at different time moments, with fixed values of α and β (chosen to correspond to typical parameters of films, as an order of magnitude). After a relatively fast initial evolution, the dimple reaches its stationary shape which does not change any longer.

Our aim is to compare the outcome of the theory with experimentally determined profiles. For that reason, we investigated oscillating dimples in a system which consisted of an aqueous solution of the non-ionic surfactant nonylphenol polyoxyethylene (40) (supplied by The Dow Chemical Company), and a styrene phase (Merck, stabilized against polymerization). This surfactant is soluble both in water and in oil. Its concentration was 1:30 parts by weight (3.23% wt, 0.0163 M). 0.1 M electrolyte, NaCl (Merck, p.a. grade), was added to the aqueous phase. We used water purified by a Milli-Q system (Millipore). Emulsion films were formed in a glass capillary immersed into the oil. The experimental method is described in detail elsewhere (9). Microscopic observations were carried out in reflected monochromatic light (wavelength 546 nm). The interference picture was recorded by videocamera, and the images were processed with the help of Targa+ 16/32P grabbing board. From the Newton fringes (see Fig. 3) we obtained the profile of the film thickness, following the method developed by Dimitrov *et al.* (20).

As the surfactant was initially dissolved in the aqueous film, it diffused across the interfaces toward the oil. The transfer induced spontaneous cyclic dimpling, with a period of the order of 1–2 min. The dimples consecutively flowed out of the film (cf. Fig. 3), and new ones formed. We monitored the time evolution taking the shapes at different moments. Let us mention here that the theory in its present form does not account for the cyclic nature of the processes, it always gives a stationary final shape. In reality, steady state dimples were observed experimentally when the film diameters were smaller than a certain limiting value (9). As a rule, if the mass fluxes are very intensive, the stationary state cannot be reached because instabilities occur in the film (see below), and the dimple is expelled at some critical size. After that a new dimple appears and that is how the oscillations come about. Nevertheless, we believe that the theory presented here describes realistically the process of dimple growth. Figure 4 shows experimental data (the large symbols) for one film with dimple. Those data were fitted with the theory by inserting the first curve as initial condition for the computation. One may estimate the film thickness along the periphery, h_0, from the intensity of the reflected light and the order of interference. Thus, $h_0 \approx 350$ nm in our case. Besides, $R = 320$ μm. Then, with $\sigma_0 = 5$ dyn/cm, and $\eta = 0.01$ g/(cm·s) for water, we can fix α according to Eq. [34]. The value of the interfacial tension, σ_0, was measured by means of du Nouy platinum ring method. As far as τ is concerned, the form of Eqs. [33] and [34] suggests that for scaling purposes we can choose an arbitrary constant with dimension of time, which is not bound to coincide with the real characteristic time of the dimpling process. Indeed, both α and β depend linearly on τ, which means that we can multiply Eq. [33] by any numerical fac-

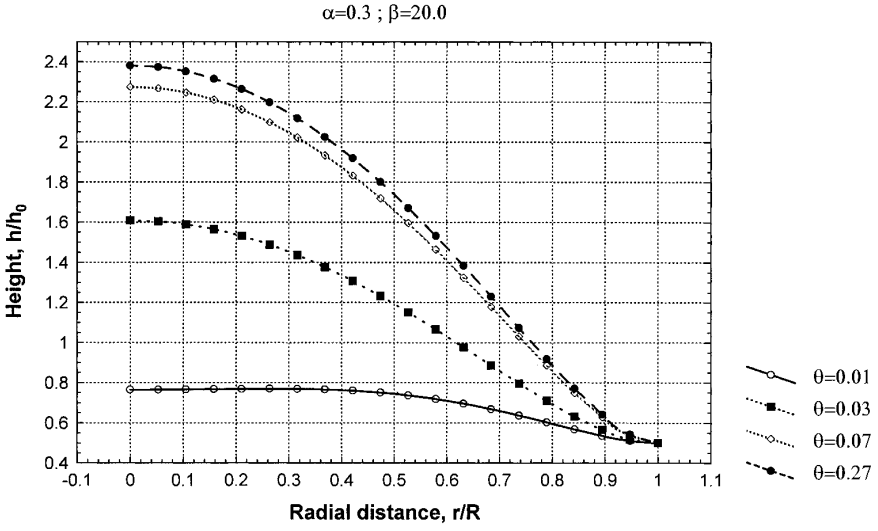

FIG. 2. Illustration of the time evolution of the dimple, calculated with the following parameters: $\alpha = 0.3$, $\beta = 20.0$.

tor, say χ, and get the same results for $H(\rho, (\theta/\chi))$. We prefer to assign large numbers to $(\chi\tau)$ because then the dimensionless time, (θ/χ), is small. This allows faster calculation with higher accuracy. Typically, $(\chi\tau) = 10^4$ s is used, and the final results are converted back to real time.

With fixed $\alpha = 0.06815$ we varied β (as an adjustable parameter) in order to obtain the best fits drawn in Fig. 4. All curves correspond to one and the same value of $\beta = 390.0$. It is seen that the agreement between theory and experiment is very good for the four time moments after the initial state. Thus, our model provides adequate description of the dimpling kinetics, using only one fitting parameter. The surfactant adsorption, Γ_0, can be determined from the isotherm of the equilibrium interfacial tension. The latter was measured by us as a function of the concentration. We assume that Γ_0 refers to saturated adsorption because the surfactant content is well above the critical micellar concentration. With $\Gamma_0 = 1.17 \times 10^{14}$ cm^{-2}, Eq. [34] yields $j_0 = 9.13 \times 10^{12}$ cm$^{-2} \cdot$ s^{-1}. This value can be used to qualitatively estimate the kinetics of saturation of emulsion drops with surfactant which has been initially dissolved in the aqueous phase. Simple assessment reveals that in an oil droplet of radius 5 μm the concentration will increase with 5.5×10^{-3} M for 1 min (if the flux remains constant). Evidently, in such a system the mass transfer is relatively fast.

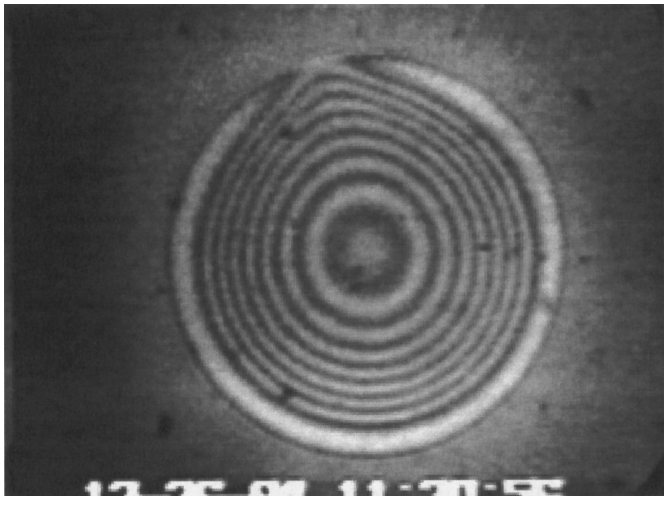

FIG. 3. Interference picture, in reflected monochromatic light, of a film containing dimple. Black and white fringes correspond to thicknesses in multiples of $\lambda/(4n)$, λ is the wavelength of the light, n is the refractive index of the aqueous phase. (The dimple just starts flowing out.)

Having found α and β, we use them to run a computation starting from initially flat film. The results are shown in Fig. 5. The first experimental profile is recovered at $t = 37.5$ s from the beginning. Thus we determine the time moment which corresponds to the first curve in Fig. 4. This time is in agreement with what was found by observation in the real system. It has to be mentioned that, actually, the dimples do not start growing from a perfectly plane-parallel film. As a matter of fact, after the preceding dimple has flown out, the surfaces remain slightly bulged, which is the real starting shape. However, at this stage the dimples are not circular and the interferometric measurements cannot be performed with sufficient accuracy.

We made some theoretical investigations of the flow properties inside the film during the non-stationary process of dimple growth. The radial velocity component on the surface, u, is a linear function of r, as is evident from Eq. [26] (the term with the molecular surface diffusion turned out to be negligible). Moreover, u has negative sign, which means that the flow near S is directed toward the film center. The vertical velocity on S, ν_z, can be obtained from Eq. [4]. Using the slope of the shape at each point, $\partial h/\partial r$, one may switch to tangential and normal velocity components with respect to S, ν_t and ν_n. These are plotted in Fig. 6 for different times after a flat initial state. The values of the parameters, α, β, are the same as in the real system (and in

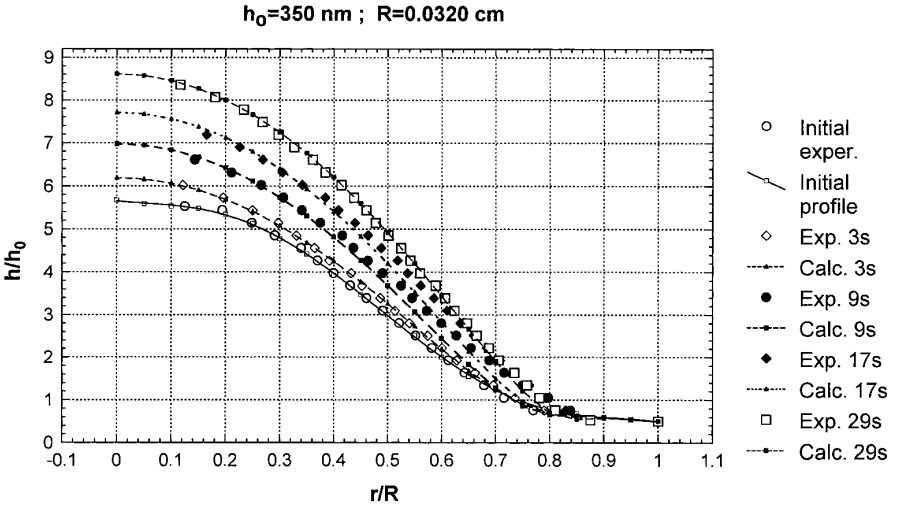

FIG. 4. Experimental and theoretical profiles of a growing dimple. $\alpha = 0.06815$, $\beta = 390.0$, $h_0 = 350$ nm, $R = 320$ μm.

Figs. 4 and 5). To define dimensionless quantities, u is scaled by R/τ and ν_z is scaled by h_0/τ. At longer times the tangential velocity increases, and the normal velocity tends to zero. This has to be expected because in stationary conditions ν_n should vanish on S. The normal motion is maximum at the film center, where the tangential velocity is always zero due to the symmetry. It is interesting to note that ν_r ($r = R$) is time independent.

We determine the pressure according to Eq. [9], discarding the term with Π. Up to the leading order, $\sigma = \sigma_0$ is assumed. One can express $q(r, t)$ in integrated form, since $p(\text{film}) = p(\text{oil})$ when the interface is flat. The present model implies that the pressure at the oil side does not depend on r. For scaling purposes we use the characteristic pressure dimension, $\eta R^2/(\tau h_0^2)$. Figure 7 shows the pressure distributions at different time moments, with the same values of the parameters as above. Generally speaking, $p(\text{film}) - p(\text{oil})$ is positive in the region where the shape of the dimple is convex (cf. profiles in Fig. 4). In addition, the pressure near the film center changes only slightly with time after, say, 40 s from the initial state. On the contrary, $p(\text{film})$ is smaller than $p(\text{oil})$ where the surface is concave, in a zone closer to the periphery. Moreover, $p(\text{film})$ decreases substantially as the stationary state is approached. This may be the reason why in the real system the dimple flows out and cannot reach a steady shape. Very high negative pressures close to the rim can induce instabilities. We have to mention also that the theory does not consider the meniscus region near the film. In reality, the contact angle is small and mass transfer takes place there, which can influence the behavior of the flow around the periphery.

Next, we compute the profile of the radial velocity inside the film as a function of the vertical coordinate. According to Eq. [6], this profile is parabolic. Data are plotted in Fig.

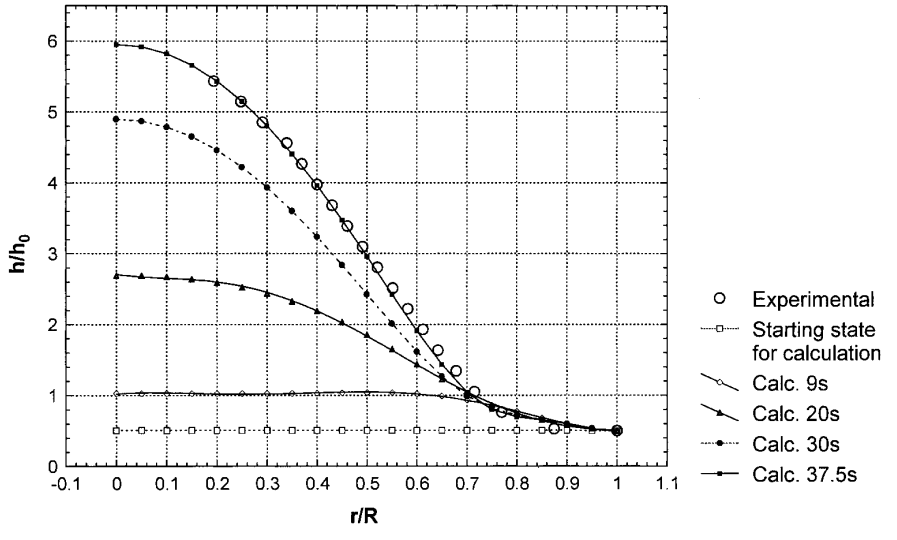

FIG. 5. Fit of the first experimental profile with computations which start from a plane-parallel film, $\alpha = 0.06815$, $\beta = 390.0$.

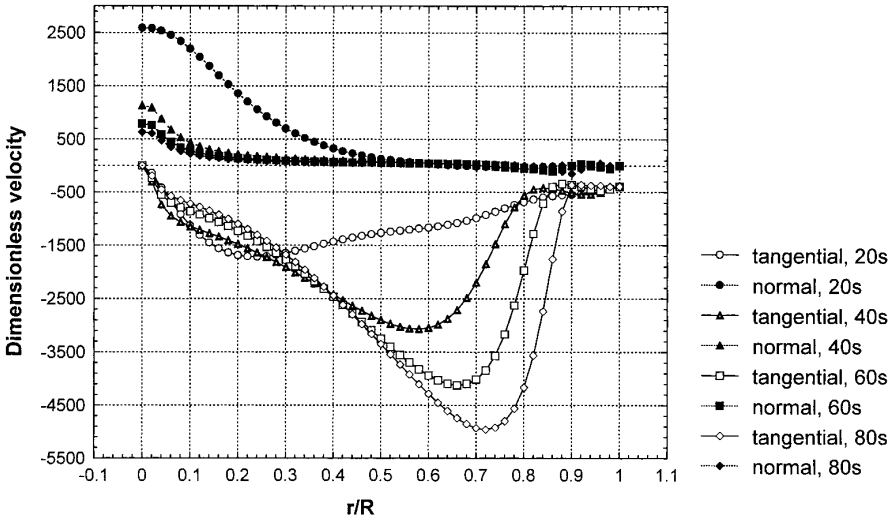

FIG. 6. Tangential and normal velocity components on the surface of the dimple at different times during its evolution (20, 40, 60, and 80 s).

8 for a given time moment, 60 s after the initial state, at four different radial distances. In other words, we take four vertical cross-sections of the film. Near the central region the velocity changes sign along the z-line. This is an important finding which proves the existence of a vortex. Indeed, the flow near the surface is directed toward the film center (negative ν_r), whereas close to the plane $z = 0$ the fluid moves to the opposite (positive ν_r). Around the film periphery the vortex disappears due to the liquid influx from the outside. This behavior is time dependent. At the early stage of the dimple growth there is no vortex at all, as the interior of the film is being filled up with fluid. Figure 9 illustrates the changes in the radial velocity at $z = 0$. Obviously, the vortex shows up after $\sim$40 s of time evolution. It occupies larger parts of the film as the dimple grows and may have a share in causing instabilities which ultimately lead to dimple expulsion. Figure 10 presents a very simplified sketch of the vortex. The drawing is not to scale (we recall that even with dimple $h/R \sim 10^{-2}$).

In the stationary state the overall liquid flux should be zero through any cylindrical surface $r = \text{const}$. More precisely,

$$\int_{z=0}^{z=h(r)} \nu_r(r = const, z)dz = 0.$$

We checked this, plotting $\nu_r(z)$ at $r/R = 0.5$ (Fig. 11), with $\alpha = 0.06815$ and $\beta = 390.0$, at time $t = 350$ s, when the dimple has supposedly become steady. From Fig. 11 we see that this is indeed so.

4. CONCLUDING REMARKS

We solved theoretically the problem for the spontaneous growth of a dimple in emulsion film with surfactant mass

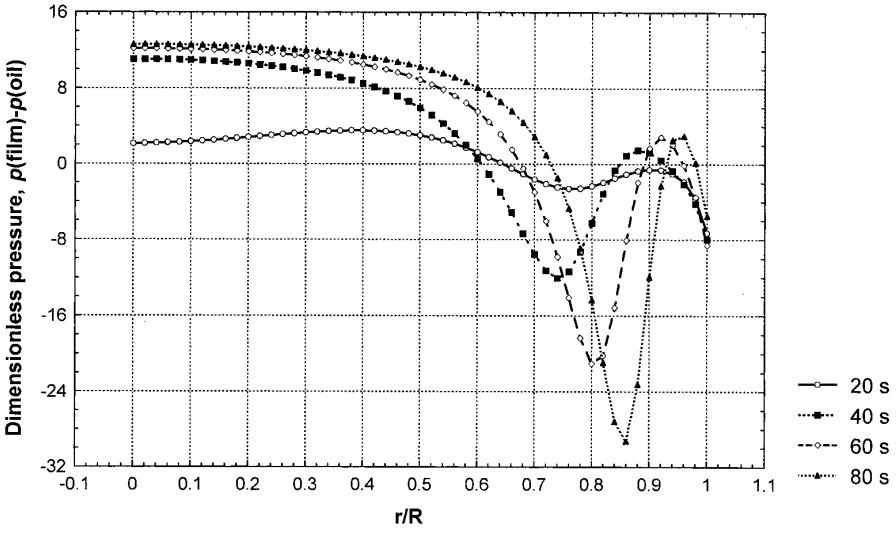

FIG. 7. Pressure distribution in the growing dimple (at 20, 40, 60, and 80 s).

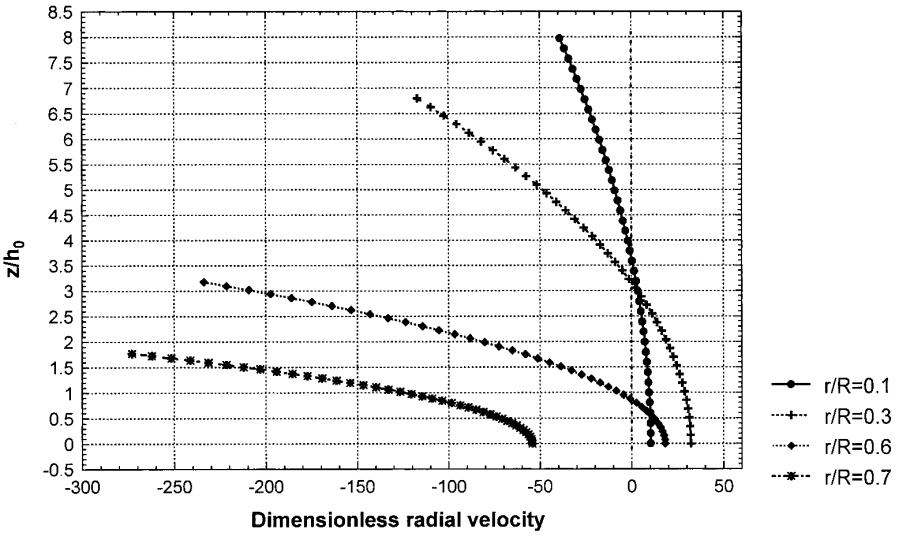

FIG. 8. Radial velocity distribution in the film, $\nu_r(z)$, 60 s after the initial state, at $r/R = 0.1$, 0.3, 0.6, and 0.7.

transfer. It has been proven that the molecular surface diffusion and the surface viscosity are insignificant for the phenomenon, in the conditions of a typical system. Moreover, the diffusion flux of surfactant from the film phase toward the interface turns out to be negligible. (The bulk diffusion coefficient, D, does not enter into the final equation for the shape, Eq. [28], and in the boundary conditions.) The surface convection, that is, the inward flow along the interfaces, directed from the meniscus to the film, provides a continuous supply of new surfactant. A major role can be attributed to the Marangoni effect, connected with *interfacial tension* gradients (see Eq. [11]) that bring about surface motion directed opposite to the *pressure* gradients (cf. Fig. 7 for p(film)). As a fluid element moves to the film center, along the interface, it continuously loses surfactant because the latter goes to the oil phase. Therefore, the surface concentration decreases and the interfacial tension rises with diminishing values of the radial coordinate, r. The occurring interfacial tension gradients set the fluid surface into motion. Thus, liquid is dragged into the film, feeding the dimple.

A differential equation which describes the time dependence of the dimple shape is formulated. Numerical computations have been performed and the results are compared with experimental data measured interferometrically. Very good agreement is observed. The main factor which affects the dynamics of the process is the surfactant flux across the interfaces, toward the oil phases. The interfacial tension, the thickness of the film, its diameter and the equilibrium adsorption are important parameters. Quasistationary shapes are possible for not very big diffusion fluxes. Otherwise, large negative pressures develop near the film periphery and eventually lead to instability in the real system. The analysis

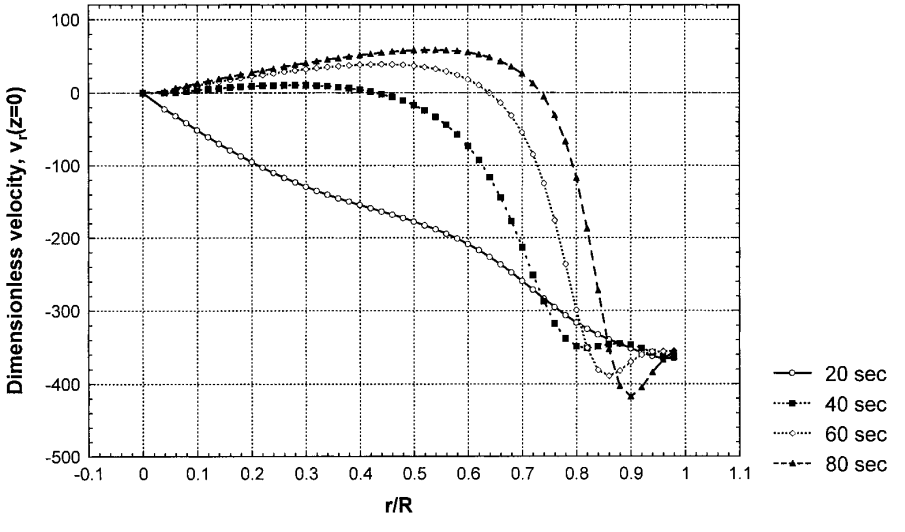

FIG. 9. Radial velocity in the plane $z = 0$, at different times (20, 40, 60, and 80 s).

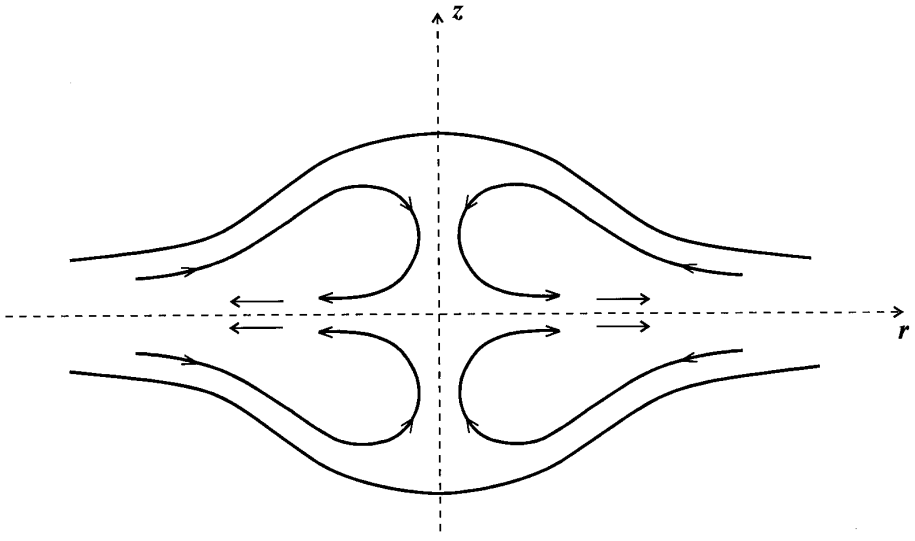

FIG. 10. Simplified sketch of the vortices in the dimple, at late stages of its time evolution (not to scale).

of the flow properties inside the film reveals the appearance of vortices which show up after a certain initial period of dimple growth.

Perhaps the most important and striking feature of these emulsion films is their thickness. Being of the order of 350 nm, and even larger, it cannot be explained by any direct surface forces. The disjoining pressure is completely negligible, especially in the presence of 0.1 mol/l of inorganic electrolyte. The stabilising effect is likely to be due to purely hydrodynamic reasons, in particular, to net repulsion when the pressure is integrated along the liquid/liquid interface.

APPENDIX

Here we outline how Eqs. [8] and [9] can be derived. In the absence of inertia effects the general form of the stress balance on S (Fig. 1) reads

$$\nabla_{\mathrm{II}} \cdot \mathbf{T}_{\mathrm{II}} + \Pi(\mathbf{n} \cdot \mathbf{e}_z)\mathbf{e}_z = \mathbf{n} \cdot (\mathbf{T}_1 - \mathbf{T}_2)|_{z=h}, \quad [A.1]$$

where ∇_{II} is the two-dimensional gradient operator on S, $\mathbf{T}_{\mathrm{II}}$ is the surface stress tensor on S, and $\mathbf{T}_1$ and $\mathbf{T}_2$ represent the bulk stress tensors in the film (subscript 1) and in the oil phase (subscript 2). In Eq. [A.1] $\mathbf{T}_1$ and $\mathbf{T}_2$ are taken at $z = h$, that is, on the surface S. $\mathbf{n}$ is the unit normal to S, directed outward from the film, $\mathbf{e}_z$ is the unit vector along the z-axis (Fig. 1). The disjoining pressure is denoted by Π, it accounts for the molecular interactions in the thin film. The term with Π in Eq. [A.1] is non-trivial, the reader may consult ref. (21) for the general derivation. In our case the form of this term corresponds to a symmetric circular film (Fig. 1); see also ref. (22).

We shall decompose Eq. [A.1] into tangential and normal projections with respect to S, using the fact that $h \ll R$. The

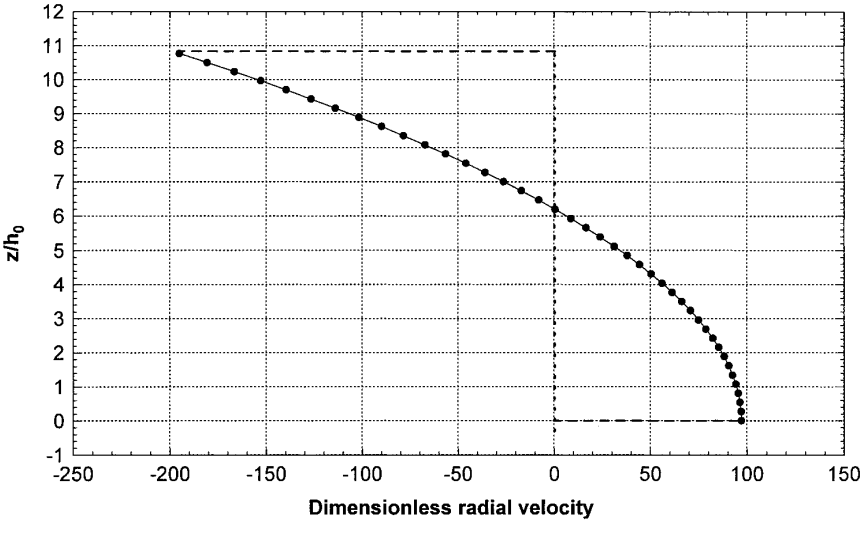

FIG. 11. Radial velocity, $\nu_r(z)$, at $r/R = 0.50$, in the stationary state of the film (at 350 s after the initial moment); $\alpha = 0.06815$, $\beta = 390.0$.

following exact relations hold between the unit vectors $\mathbf{n}$, $\mathbf{e}_t$, $\mathbf{e}_r$, and $\mathbf{e}_z$ (Fig. 1):

$$\mathbf{n} = \frac{1}{\sqrt{1 + (\partial h/\partial r)^2}} \left(- \frac{\partial h}{\partial r} \mathbf{e}_r + \mathbf{e}_z \right);$$

$$\mathbf{e}_t = \frac{1}{\sqrt{1 + (\partial h/\partial r)^2}} \left(\mathbf{e}_r + \frac{\partial h}{\partial r} \mathbf{e}_z \right). \qquad [A.2]$$

We keep the leading order terms only, which is equivalent to setting $\partial h/\partial r \to 0$ in [A.2] (vanishingly small slope of S); in this approximation $\mathbf{n} \equiv \mathbf{e}_z$, and the vector tangential to S, $\mathbf{e}_t$, coincides with $\mathbf{e}_r$, i.e., with the unit vector along the radial axis Or (Fig. 1).

For the surface stress tensor one writes

$$\mathbf{T}_{II} = \sigma \mathbf{U}_{II} + \eta_d (\nabla_{II} \cdot \mathbf{v}_S) \mathbf{U}_{II} + 2\eta_{sh} \times \left[\mathbf{D} - \frac{1}{2} (\nabla_{II} \cdot \mathbf{v}_S) \mathbf{U}_{II} \right], \qquad [A.3]$$

hereby including the contributions of dilatational and shear surface viscosities, η_d and η_{sh}; see refs. (8, 23). σ is the interfacial tension, $\mathbf{v}_S$ is the velocity on S, $\mathbf{U}_{II}$ stands for the two-dimensional unit tensor on S, and $\mathbf{D}$ is the surface rate-of-strain tensor:

$$\mathbf{D} = \frac{1}{2} \mathbf{U}_{II} \cdot [(\nabla_{II} \mathbf{v}_S) + (\nabla_{II} \mathbf{v}_S)\dagger] \cdot \mathbf{U}_{II} \qquad [A.4]$$

The symbol ''†'' means transposition. In the two volume phases adjacent to S the bulk stress tensors, $\mathbf{T}_k$, obey the equations

$$\mathbf{T}_k = -p_k \mathbf{U} + \eta_k [(\nabla \mathbf{v}_k) + (\nabla \mathbf{v}_k)\dagger], \; k = 1, 2. \qquad [A.5]$$

p_1, p_2, η_1, η_2, $\mathbf{v}_1$, and $\mathbf{v}_2$ are, respectively, the pressures, the viscosities, and the velocities in the phases 1 and 2; $\mathbf{U}$ and ∇ are the three-dimensional unit tensor and gradient operator. From the side of the oil phase the viscous stresses applied on S are negligible, and the change of p_2 in radial direction can be ignored (see the main text). Therefore, for $k = 2$, Eq. [A.5] gives

$$\mathbf{T}_2 = -p_2 \mathbf{U}; \; p_2 = \text{const.} \qquad [A.6]$$

It is now straightforward to insert Eqs. [A.3]–[A.6] into [A.1]. The projection of Eq. [A.1] along $\mathbf{e}_r$ leads to Eq. [8], and the $\mathbf{e}_z$ projection yields Eq. [9]. For the sake of brevity the subscript 1 is omitted in the main text.

ACKNOWLEDGMENT

This work was financially supported by DOW Deutschland, Inc., and in part by the Bulgarian Ministry of Education, Science and Technologies.

REFERENCES

1. Ivanov, I. B., Chakarova, Sv. K., and Dimitrova, B. I., *Colloids Surfaces* **22,** 311 (1987).
2. Dimitrova, B. I., Ivanov, I. B., and Nakache, E., *J. Dispersion Sci. Technol.* **9,** 321 (1988).
3. Sternling, C. V., and Scriven, L. E., *AIChE J.* **5,** 514 (1959).
4. Davies, J. T., and Rideal, E. K., ''Interfacial Phenomena.'' Academic Press, New York, 1963.
5. Velev, O. D., Gurkov, T. D., Ivanov, I. B., and Borwankar, R., *Phys. Rev. Lett.* **75,** 264 (1995).
6. Fisher, L. R., and Parker, N. S., *Biophys. J.* **46,** 253 (1984).
7. Hartland, S., Coalescence in Dense-Packed Dispersions, *in* ''Thin Liquid Films'' (I. B. Ivanov, Ed.), Chapter 10, p. 663. Marcel Dekker, New York, 1988.
8. Edwards, D. A., Brenner, H., and Wasan, D. T., ''Interfacial Transport Processes and Rheology.'' Butterworth–Heinemann, Boston, 1991.
9. Velev, O. D., Gurkov, T. D., and Borwankar, R. P., *J. Colloid Interface Sci.* **159,** 497 (1993).
10. Frankel, S. P., and Mysels, K. J., *J. Phys. Chem.* **66,** 190 (1962).
11. Ivanov, I. B., and Dimitrov, D. S., Thin Film Drainage, *in* ''Thin Liquid Films'' (I. B. Ivanov, Ed.), Chapter 7, p. 379. Marcel Dekker, New York, 1988.
12. Hartland, S., Yang, B., and Jeelani, S. A. K., *Chem. Eng. Sci.* **49,** 1313 (1994).
13. Landau, L. D., and Lifshitz, E. M., ''Fluid Mechanics.'' Pergamon Press, Oxford, 1984.
14. Stokes, G. G., *Trans. Cambridge Philos. Soc.* **9,** 8 (1851).
15. Lord Rayleigh, *Phil. Mag.* **21,** 697 (1911).
16. Ivanov, I. B., and Traykov, T. T., *Int. J. Multiphase Flow* **2,** 397 (1976).
17. Traykov, T. T., and Ivanov, I. B., *Int. J. Multiphase Flow* **3,** 471 (1977).
18. Ivanov, I. B., *Pure Appl. Chem.* **52,** 1241 (1980).
19. Constantinides, A., ''Applied Numerical Methods with Personal Computers.'' McGraw-Hill, New York, 1987.
20. Dimitrov, A. S., Kralchevsky, P. A., Nikolov, A. D., and Wasan, D. T., *Colloids Surfaces* **47,** 299 (1990).
21. Kralchevsky, P. A., and Ivanov, I. B., *J. Colloid Interface Sci.* **137,** 234 (1990).
22. Kralchevsky, P. A., Paunov, V. N., Denkov, N. D., and Nagayama, K., *J. Chem. Soc. Faraday Trans.* **91,** 3415 (1995).
23. Slattery, J. C., ''Interfacial Transport Phenomena.'' Springer-Verlag, New York, 1990.